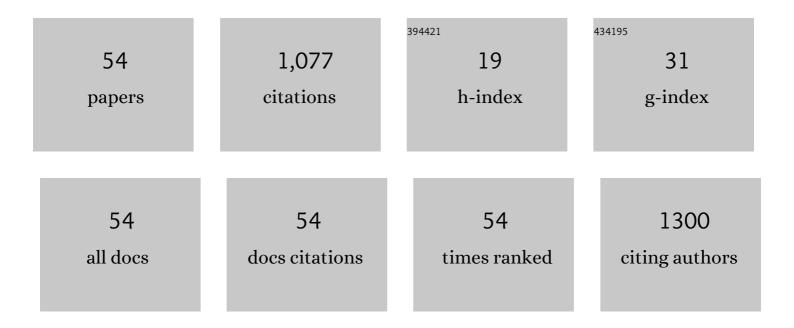
## **Christoph Vogler**

List of Publications by Year in descending order

Source: https://exaly.com/author-pdf/9144149/publications.pdf Version: 2024-02-01



#	Article	IF	CITATIONS
1	3D print of polymer bonded rare-earth magnets, and 3D magnetic field scanning with an end-user 3D printer. Applied Physics Letters, 2016, 109, .	3.3	168
2	3D Printing of Polymer-Bonded Rare-Earth Magnets With a Variable Magnetic Compound Fraction for a Predefined Stray Field. Scientific Reports, 2017, 7, 9419.	3.3	80
3	Topologically protected vortex structures for low-noise magnetic sensors with high linear range. Nature Electronics, 2018, 1, 362-370.	26.0	60
4	Heat-assisted magnetic recording of bit-patterned media beyond 10 Tb/in2. Applied Physics Letters, 2016, 108, .	3.3	53
5	A three-dimensional spin-diffusion model for micromagnetics. Scientific Reports, 2015, 5, 14855.	3.3	51
6	Topology optimized and 3D printed polymer-bonded permanent magnets for a predefined external field. Journal of Applied Physics, 2017, 122, .	2.5	51
7	A self-consistent spin-diffusion model for micromagnetics. Scientific Reports, 2016, 6, 16.	3.3	40
8	Landau-Lifshitz-Bloch equation for exchange-coupled grains. Physical Review B, 2014, 90, .	3.2	35
9	3D FEM–BEM-coupling method to solve magnetostatic Maxwell equations. Journal of Magnetism and Magnetic Materials, 2012, 324, 1862-1866.	2.3	30
10	Dipolar-stabilized first and second-order antiskyrmions in ferrimagnetic multilayers. Nature Communications, 2021, 12, 2611.	12.8	29
11	Fundamental limits in heat-assisted magnetic recording and methods to overcome it with exchange spring structures. Journal of Applied Physics, 2015, 117, 163913.	2.5	28
12	Spin Torque Efficiency and Analytic Error Rate Estimates of Skyrmion Racetrack Memory. Scientific Reports, 2019, 9, 4827.	3.3	26
13	Magnetoelastic resonance sensor for remote strain measurements. Applied Physics Letters, 2012, 101, 042402.	3.3	24
14	Simulating rare switching events of magnetic nanostructures with forward flux sampling. Physical Review B, 2013, 88, .	3.2	24
15	Solving Large-Scale Inverse Magnetostatic Problems using the Adjoint Method. Scientific Reports, 2017, 7, 40816.	3.3	24
16	Calculation of coercivity of magnetic nanostructures at finite temperatures. Physical Review B, 2011, 84, .	3.2	22
17	Thermal switching field distribution of a single domain particle for field-dependent attempt frequency. Journal of Applied Physics, 2012, 112, 023903.	2.5	22
18	Areal density optimizations for heat-assisted magnetic recording of high-density media. Journal of Applied Physics, 2016, 119, .	2.5	20

CHRISTOPH VOGLER

#	Article	IF	CITATIONS
19	Fieldlike and Dampinglike Spin-Transfer Torque in Magnetic Multilayers. Physical Review Applied, 2017, 7, .	3.8	20
20	Back-Hopping in Spin-Transfer-Torque Devices: Possible Origin and Countermeasures. Physical Review Applied, 2018, 9, .	3.8	18
21	A repulsive skyrmion chain as a guiding track for a racetrack memory. AIP Advances, 2018, 8, .	1.3	16
22	Large scale finite-element simulation of micromagnetic thermal noise. Journal of Magnetism and Magnetic Materials, 2019, 475, 408-414.	2.3	16
23	Combining micromagnetism and magnetostatic Maxwell equations for multiscale magnetic simulations. Journal of Magnetism and Magnetic Materials, 2013, 343, 163-168.	2.3	15
24	A fast finite-difference algorithm for topology optimization of permanent magnets. Journal of Applied Physics, 2017, 122, .	2.5	15
25	Thermally superactive artificial kagome spin ice structures obtained with the interfacial Dzyaloshinskii-Moriya interaction. Physical Review B, 2020, 102, .	3.2	15
26	Basic noise mechanisms of heat-assisted-magnetic recording. Journal of Applied Physics, 2016, 120, .	2.5	13
27	Calculating thermal stability and attempt frequency of advanced recording structures without free parameters. Journal of Applied Physics, 2015, 117, 163907.	2.5	12
28	Dependence of energy barrier reduction on collective excitations in square artificial spin ice: A comprehensive comparison of simulation techniques. Physical Review B, 2020, 102, .	3.2	11
29	A full-fledged micromagnetic code in fewer than 70 lines of NumPy. Journal of Magnetism and Magnetic Materials, 2015, 387, 13-18.	2.3	10
30	Stochastic ferrimagnetic Landau-Lifshitz-Bloch equation for finite magnetic structures. Physical Review B, 2019, 100, .	3.2	10
31	Noise Reduction Based on an Feâ^'Rh Interlayer in Exchange-Coupled Heat-Assisted Recording Media. Physical Review Applied, 2017, 8, .	3.8	9
32	Hybrid FFT algorithm for fast demagnetization field calculations on non-equidistant magnetic layers. Journal of Magnetism and Magnetic Materials, 2020, 503, 166592.	2.3	8
33	Passive wireless strain measurement based upon the Villari effect and giant magnetoresistance. Applied Physics Letters, 2016, 109, .	3.3	7
34	Contactless and absolute linear displacement detection based upon 3D printed magnets combined with passive radio-frequency identification. AIP Advances, 2017, 7, .	1.3	7
35	Efficient micromagnetic modelling of spin-transfer torque and spin-orbit torque. AIP Advances, 2018, 8, .	1.3	7
36	GPU-Accelerated Atomistic Energy Barrier Calculations of Skyrmion Annihilations. IEEE Transactions on Magnetics, 2018, 54, 1-5.	2.1	7

CHRISTOPH VOGLER

#	Article	IF	CITATIONS
37	Microscopic Origin of Magnetization Reversal in Nanoscale Exchange-Coupled Ferri/Ferromagnetic Bilayers: Implications for High Energy Density Permanent Magnets and Spintronic Devices. ACS Applied Nano Materials, 2020, 3, 9218-9225.	5.0	7
38	Macroscopic simulation of isotropic permanent magnets. Journal of Magnetism and Magnetic Materials, 2016, 401, 875-879.	2.3	6
39	Noise reduction in heat-assisted magnetic recording of bit-patterned media by optimizing a high/low Tc bilayer structure. Journal of Applied Physics, 2017, 122, .	2.5	6
40	Spin-Canting Effects in GMR Sensors With Wide Dynamic Field Range. IEEE Sensors Journal, 2021, 21, 13176-13183.	4.7	6
41	Influence of grain size and exchange interaction on the LLB modeling procedure. Journal of Applied Physics, 2016, 120, 223903.	2.5	5
42	Significant reduction of critical currents in MRAM designs using dual free layer with perpendicular and in-plane anisotropy. Applied Physics Letters, 2017, 110, .	3.3	5
43	Systematic parameterization of heat-assisted magnetic recording switching probabilities and the consequences for the resulting SNR. Journal of Applied Physics, 2019, 126, .	2.5	5
44	Removal of earth's magnetic field effect on magnetoelastic resonance sensors by an antisymmetric bias field. Sensors and Actuators A: Physical, 2012, 183, 11-15.	4.1	4
45	Fully coupled, dynamic model of a magnetostrictive amorphous ribbon and its validation. Journal of Applied Physics, 2014, 115, .	2.5	4
46	Reactivable passive radio-frequency identification temperature indicator. Journal of Applied Physics, 2015, 117, .	2.5	4
47	Efficiently reducing transition curvature in heat-assisted magnetic recording with state-of-the-art write heads. Applied Physics Letters, 2017, 110, 182406.	3.3	4
48	Curie temperature modulated structure to improve the performance in heat-assisted magnetic recording. Journal of Magnetism and Magnetic Materials, 2019, 474, 442-447.	2.3	4
49	Hysteresis-free magnetization reversal of exchange-coupled bilayers with finite magnetic anisotropy. Physical Review B, 2020, 102, .	3.2	4
50	Three-dimensional magneto-resistive random access memory devices based on resonant spin-polarized alternating currents. Journal of Applied Physics, 2011, 109, 123901.	2.5	3
51	Statistical analysis of read-back signals in magnetic recording on granular media. AIP Advances, 2020, 10, 015307.	1.3	3
52	Ultra-Low-Cost RFID Based on Soft Magnetic Ribbons. IEEE Transactions on Magnetics, 2014, 50, 1-5.	2.1	2
53	Superior bit error rate and jitter due to improved switching field distribution in exchange spring magnetic recording media. Scientific Reports, 2016, 6, 27048.	3.3	2

54 The influence of spin-diffusion effects on current driven domain-wall motion. , 2015, , .

0